



Published in final edited form as:

Stroke. 2014 August ; 45(8): 2475–2479. doi:10.1161/STROKEAHA.114.005079.

Acute and Delayed Deferoxamine Treatment Attenuates Long-Term Sequelae after Germinal Matrix Hemorrhage in Neonatal Rats

Damon Klebe, BA, Paul R. Krafft, MD, Clotilde Hoffmann, BS, Tim Lekic, MD, PhD, Jerry J. Flores, BS, William Rolland, BS, and John H. Zhang, MD, PhD

Department of Physiology & Pharmacology, Loma Linda University School of Medicine, Loma Linda, California, USA

Abstract

Background and Purpose—This study investigated if acute and delayed Deferoxamine treatment attenuates long-term sequelae after germinal matrix hemorrhage (GMH).

Methods—Bacterial collagenase (0.3 U) was infused intraparenchymally into the right hemispheric ganglionic eminence in P7 rat pups to induce GMH. GMH animals received either Deferoxamine or vehicle twice a day for 7 consecutive days. Deferoxamine administration was initiated at either 1 hour or 72 hours post-GMH. Long-term neurocognitive deficits and motor coordination were assessed using Morris water maze, rotarod, and foot fault tests between day 21–28 post-GMH. At 28 days post-GMH, brain morphology was assessed and extracellular matrix protein (fibronectin and vitronectin) expression was determined.

Results—Acute and delayed Deferoxamine treatment improved long-term motor and cognitive function at 21–28 days post-GMH. Attenuated neurofunction was paralleled with improved overall brain morphology at 28 days post-GMH, reducing white matter loss, basal ganglia loss, post-hemorrhagic ventricular dilation, and cortical loss. GMH resulted in significantly increased expression of fibronectin and vitronectin, which was reversed by acute and delayed Deferoxamine treatment.

Conclusion—Acute and delayed Deferoxamine administration ameliorated long-term sequelae after GMH.

Keywords

Deferoxamine; Germinal Matrix Hemorrhage; Neonatal Rat; Post-Hemorrhagic Ventricular Dilation; Extracellular Matrix Proteins

Corresponding author: John H. Zhang, MD, PhD; Department of Physiology & Pharmacology, Loma Linda University, Loma Linda, California, 92354, USA, Phone: 909-558-4723, Fax: 909-558-0119, johnzhang3910@yahoo.com.

Disclosures: None

Introduction

Germinal matrix hemorrhage (GMH) occurs when immature blood vessels rupture within the subventricular tissue in premature infants.¹ GMH occurs in approximately 12000 live births per every year in the US and often results in developmental delays, mental retardation, cerebral palsy, and post-hemorrhagic hydrocephalus, posing significant socioeconomic burdens.^{1,2} Because current clinical management is limited, research is needed to investigate innovative therapeutic modalities.

In adult rodent intracerebral hemorrhage and subarachnoid hemorrhage models, red blood cells present in the intraparenchymal tissue are lysed and hemoglobin metabolized to release iron, resulting in a highly oxidative environment and consequent iron toxicity that damages brain tissue.^{3,4} Chelation of iron using Deferoxamine improved neurofunctional outcomes after intracerebral hemorrhage and subarachnoid hemorrhage, yet its efficacy has not been evaluated after neonatal GMH.^{5,6} Blood products and proliferation of extracellular matrix proteins are theorized to disrupt CSF flow dynamics following hemorrhage, leading to consequent post-hemorrhagic hydrocephalus development.⁷

We hypothesized acute and delayed Deferoxamine treatment will ameliorate extracellular matrix protein proliferation, post-hemorrhagic ventricular dilation, and long-term neurofunctional outcomes after GMH.

Methods

All protocols and procedures were approved by the Institutional Animal Care and Use Committee at Loma Linda University. The online-only Data Supplement contains detailed methods. Stereotaxic infusion of 0.3 U bacterial collagenase into the right ganglionic eminence was performed to induce GMH in P7 rat pups, as described.⁸ While some consider P7 rat pups to be equivalent in brain development of a term human infant, recent evidence suggests P7 is closer in brain development to 30–32 week gestation age human infants, which is approximately the point we want to model GMH.⁸ Forty animals were divided into four groups: Sham, Vehicle (PBS intraperitoneally BID starting 1 hour post-GMH for 7 days), acute Deferoxamine (100 mg/kg intraperitoneally BID starting 1 hour post-GMH for 7 days), and delayed Deferoxamine (100 mg/kg intraperitoneally BID starting 72 hours post-GMH for 7 days). Each animal group was alternated when undergoing surgeries.

Neurocognitive deficits and motor coordination were evaluated by Morris water maze, rotarod, and foot fault tests between 21–28 days post-GMH (n=10/group). Animals that failed to swim or only swam in stationary circles were excluded from further analysis in our study. Ventricular volume, cortical thickness, white matter loss, and basal ganglia loss were calculated in Nissl stained histological brain sections 28 days post-GMH using NIH Image J software (n=5/group). Cerebral structure borders were delineated using previously defined criteria from stereologic neuroanatomical studies using optical dissector principles^{9,10}. Volumes were calculated as the average delineated area from 10 μ m sections taken at approximately 2.5 mm, 1.2mm, 0.7 mm rostral and 2.9 mm caudal of bregma multiplied by the depth of the cerebroventricular system. Fibronectin and vitronectin expressions were

quantified by Western blot at 28 days post-GMH (n=5/group). Blinded investigators performed the neurobehavioral, histological, and Western blot analyses.

Sample size estimations were made by power analysis using a type I error rate of 0.05 and a power of 0.8 on a two-sided test. Data are expressed as mean±SEM. Western blot and histological data were analyzed by one-way ANOVA followed by the Tukey post-hoc test, and behavior data were analyzed by one-way ANOVA on ranks and the Student-Newman-Keuls method. A *P* value <0.05 was considered statistically significant.

Results

Deferoxamine Improved Brain Morphology after GMH

At 28 days post-GMH, brain morphology was assessed in Nissl stained brain sections (n=5 group). Ventricular volume was found significantly increased in the vehicle group compared to sham, but acute and delayed Deferoxamine treatment significantly reduced GMH-induced ventricular dilation (*P*<0.05; Figure 1A). Cortical thickness was evaluated as a right hemisphere/left hemisphere ratio to the mean of sham and was significantly decreased in the vehicle group compared to sham-operated animals, but acute and delayed Deferoxamine treatment ameliorated cortical loss (*P*<0.05, Figure 1B). Basal ganglia volume was evaluated as a percentage to mean sham basal ganglia volume (Figure 1C). Acute and delayed Deferoxamine treated groups had significantly less basal ganglia loss compared to the vehicle group (*P*<0.05; Figure 1C). White matter loss was evaluated as a percent loss using sham-operated animals as a baseline (Figure 1D). Acute and delayed Deferoxamine treated groups had significantly less white matter loss compared to the vehicle group (*P*<0.05; Figure 1D).

Deferoxamine Reduced Extracellular Matrix Protein Expression after GMH

Western blot analyses were conducted at 28 days post-GMH induction (n=5 per group). Fibronectin expression was found increased in the vehicle group compared to sham-operated animals, and acute and delayed Deferoxamine treatment significantly reduced fibronectin expression after GMH (*P*<0.05; Figure 2A). Vitronectin expression was also significantly increased in the vehicle group compared to sham-operated animals, and acute and delayed Deferoxamine treatment tended to reduce vitronectin expression after GMH (*P*>0.05 vs sham; Figure 2B).

Deferoxamine Improved Long-term Neurofunctional Outcomes after GMH

Vehicle treated GMH animals demonstrated significant spatial memory loss compared to sham-operated animals in the Morris water maze by swimming greater distances finding the platform (*P*<0.05; Figure 3A) and spending less time in the target quadrant during the probe trials (*P*<0.05; Figure 3B). Acute and delayed treatment animals showed significant cognitive functional recovery by having reduced swimming distances (*P*<0.05; Figure 3A) and tended to spend more time in the target quadrant during the probe trials (*P*>0.05 vs sham; Figure 3B). Furthermore, vehicle animals had significantly more foot faults than sham, but acute and delayed Deferoxamine treated GMH animals had significantly reduced foot faults compared to vehicle (*P*<0.05; Figure 3C). Vehicle animals had significantly

worse rotarod performances compared to sham, but acute and delayed Deferoxamine treated animals had significantly better rotarod performances than vehicle rats ($P < 0.05$; Figure 3D).

Discussion

Iron toxicity is known to play a crucial pathophysiological role in brain injury following hemorrhage, with some evidence indicating iron overload may contribute to hydrocephalus development.^{3, 4, 11} Blood products and extracellular matrix protein proliferation are thought to significantly contribute to post-hemorrhagic hydrocephalus development by disrupting normal cerebrospinal fluid flow in the ventricles.⁷ Deferoxamine treatment attenuated brain injury in adult brain hemorrhage models,^{5, 6} yet it has not been evaluated in neonates nor has it been shown to significantly attenuate neonatal post-hemorrhagic hydrocephalus development and long-term neurofunctional deficits. This study evaluated the efficacy of 1 hour (acute) and 72 hour (delayed) Deferoxamine treatment as a potential therapeutic modality for GMH-induced brain injury, the delayed time point serving as a more clinically relevant treatment regimen. Extracellular matrix protein proliferation is indicative of gliosis and is hypothesized to deposit within the ventricles, disrupting cerebrospinal fluid flow and contributing to post-hemorrhagic hydrocephalus development. Fibronectin and vitronectin were significantly increased in GMH animals compared to sham-operated animals, yet acute and delayed Deferoxamine treated animals had significantly reduced fibronectin and vitronectin expressions compared to vehicle, indicating GMH leads to increased extracellular matrix protein proliferation, which was attenuated by iron chelation.

Additionally, vehicle treated GMH animals demonstrated significantly enlarged ventricular volume, decreased cortical thickness, increased basal ganglia loss, and increased white matter loss, while acute and delayed Deferoxamine treated animals showed significantly improved brain morphological outcomes across all measures. Consequently, acute and delayed Deferoxamine treated GMH animals had significantly improved spatial memory and motor coordination compared to vehicle animals. Our results corroborate with similar brain hemorrhage animal models depicting Deferoxamine treatment ameliorates post-hemorrhage brain injury. Furthermore, acute and delayed post-GMH iron chelation significantly reduced neonatal post-hemorrhagic ventricular dilation.

Our results suggest that iron toxicity at acute and delayed time points following GMH is associated with post-hemorrhagic ventricular dilation, but the pathophysiological mechanisms remain to be elucidated. The choroid plexus is an epithelial layer in the ventricles specialized for cerebrospinal fluid production and is susceptible to injury following hemorrhage.¹² It also contains high expression levels of iron metabolic proteins relative to other brain tissues.¹³ Iron-overload in the cerebroventricular system following GMH may adversely affect normal functioning of the choroid plexus, leading to pathologically increased cerebrospinal fluid production. Another possible explanation is GMH-induced cerebroventricular iron overload destroys subarachnoid granulations, as is observed in subarachnoid hemorrhage, reducing overall cerebrospinal fluid reabsorption.¹⁴ Further investigations are needed to determine mechanisms linking GMH-induced iron toxicity with long-term post-hemorrhagic ventricular dilation.

Our study is the first to show Deferoxamine attenuates long-term neurocognitive and sensorimotor deficits, improves overall brain morphology, and reduces post-hemorrhagic ventricular dilation following GMH when treatment is initiated as late as 72 hours post-ictus in neonates, providing evidence for a potentially clinically translatable therapeutic modality.

Supplementary Material

Refer to Web version on PubMed Central for supplementary material.

Acknowledgments

Sources of Funding: This research was supported by the NIH (R01 NS078755 to Dr. John H. Zhang).

References

1. Ballabh P. Intraventricular hemorrhage in premature infants: Mechanism of disease. *Pediatric research*. 2010; 67:1–8. [PubMed: 19816235]
2. Kochanek KD, Kirmeyer SE, Martin JA, Strobino DM, Guyer B. Annual summary of vital statistics: 2009. *Pediatrics*. 2012; 129:338–348. [PubMed: 22291121]
3. Lee JY, Keep RF, He Y, Sagher O, Hua Y, Xi G. Hemoglobin and iron handling in brain after subarachnoid hemorrhage and the effect of deferoxamine on early brain injury. *Journal of cerebral blood flow and metabolism*. 2010; 30:1793–1803. [PubMed: 20736956]
4. Xiong, XY.; Wang, J.; Qian, ZM.; Yang, QW. [12 January 2014] Iron and intracerebral hemorrhage: From mechanism to translation. [21 December 2013]. *Translational stroke research*. 2013. <http://link.springer.com/article/10.1007%2Fs12975-013-0317-7/fulltext.html>
5. Hatakeyama T, Okauchi M, Hua Y, Keep RF, Xi G. Deferoxamine reduces neuronal death and hematoma lysis after intracerebral hemorrhage in aged rats. *Translational stroke research*. 2013; 4:546–553. [PubMed: 24187595]
6. Lee JY, Keep RF, Hua Y, Ernestus RI, Xi G. Deferoxamine reduces early brain injury following subarachnoid hemorrhage. *Acta neurochirurgica Supplement*. 2011; 112:101–106. [PubMed: 21691996]
7. Crews L, Wyss-Coray T, Masliah E. Insights into the pathogenesis of hydrocephalus from transgenic and experimental animal models. *Brain pathology*. 2004; 14:312–316. [PubMed: 15446587]
8. Lekic T, Manaenko A, Rolland W, Krafft PR, Peters R, Hartman RE, et al. Rodent neonatal germinal matrix hemorrhage mimics the human brain injury, neurological consequences, and post-hemorrhagic hydrocephalus. *Experimental neurology*. 2012; 236:69–78. [PubMed: 22524990]
9. Ekinci N, Acer N, Akkaya A, Sankur S, Kabadayi T, Sahin B. Volumetric evaluation of the relations among the cerebrum, cerebellum and brain stem in young subjects: A combination of stereology and magnetic resonance imaging. *Surgical and radiologic anatomy: SRA*. 2008; 30:489–494. [PubMed: 18478176]
10. Oorschot DE. Total number of neurons in the neostriatal, pallidal, subthalamic, and substantia nigral nuclei of the rat basal ganglia: A stereological study using the cavalieri and optical disector methods. *The Journal of comparative neurology*. 1996; 366:580–599. [PubMed: 8833111]
11. Chen Z, Gao C, Hua Y, Keep RF, Muraszko K, Xi G. Role of iron in brain injury after intraventricular hemorrhage. *Stroke*. 2011; 42:465–470. [PubMed: 21164132]
12. Simard PF, Tosun C, Melnichenko L, Ivanova S, Gerzanich V, Simard JM. Inflammation of the choroid plexus and ependymal layer of the ventricle following intraventricular hemorrhage. *Translational stroke research*. 2011; 2:227–231. [PubMed: 21731590]
13. Rouault TA, Zhang DL, Jeong SY. Brain iron homeostasis, the choroid plexus, and localization of iron transport proteins. *Metabolic brain disease*. 2009; 24:673–684. [PubMed: 19851851]
14. Okubo S, Strahle J, Keep RF, Hua Y, Xi G. Subarachnoid hemorrhage-induced hydrocephalus in rats. *Stroke*. 2013; 44:547–550. [PubMed: 23212164]

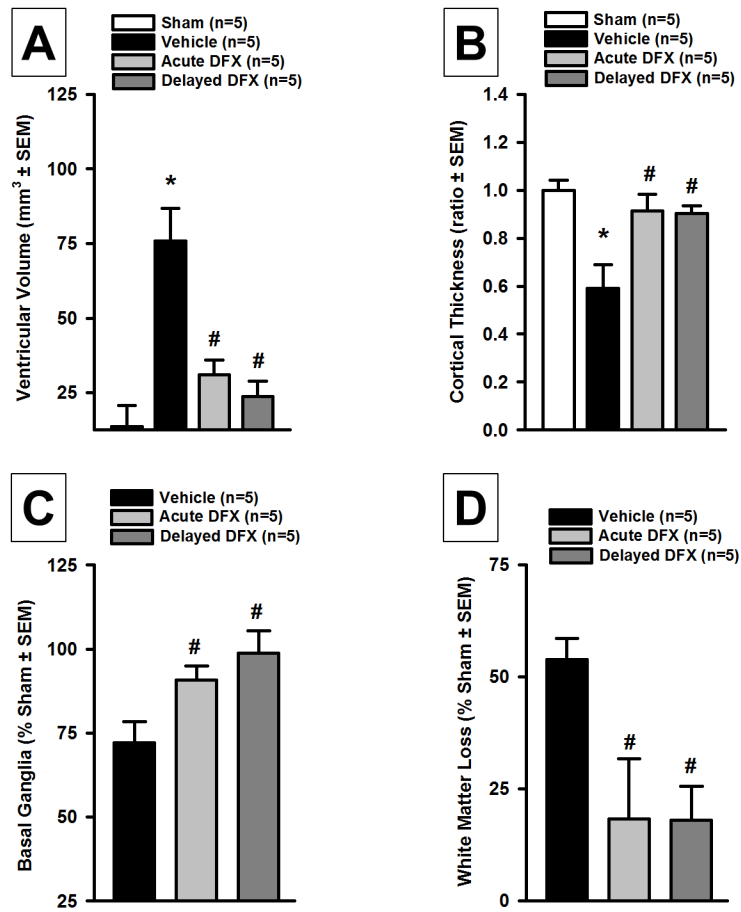


Figure 1. Quantification of (A) ventricular volume, (B) cortical thickness, (C) basal ganglia loss, and (D) white matter loss at 28 days after germinal matrix hemorrhage. Values are expressed as mean±SEM. *P<0.05 compared to sham, and #P<0.05 compared to vehicle. N=5 per group.

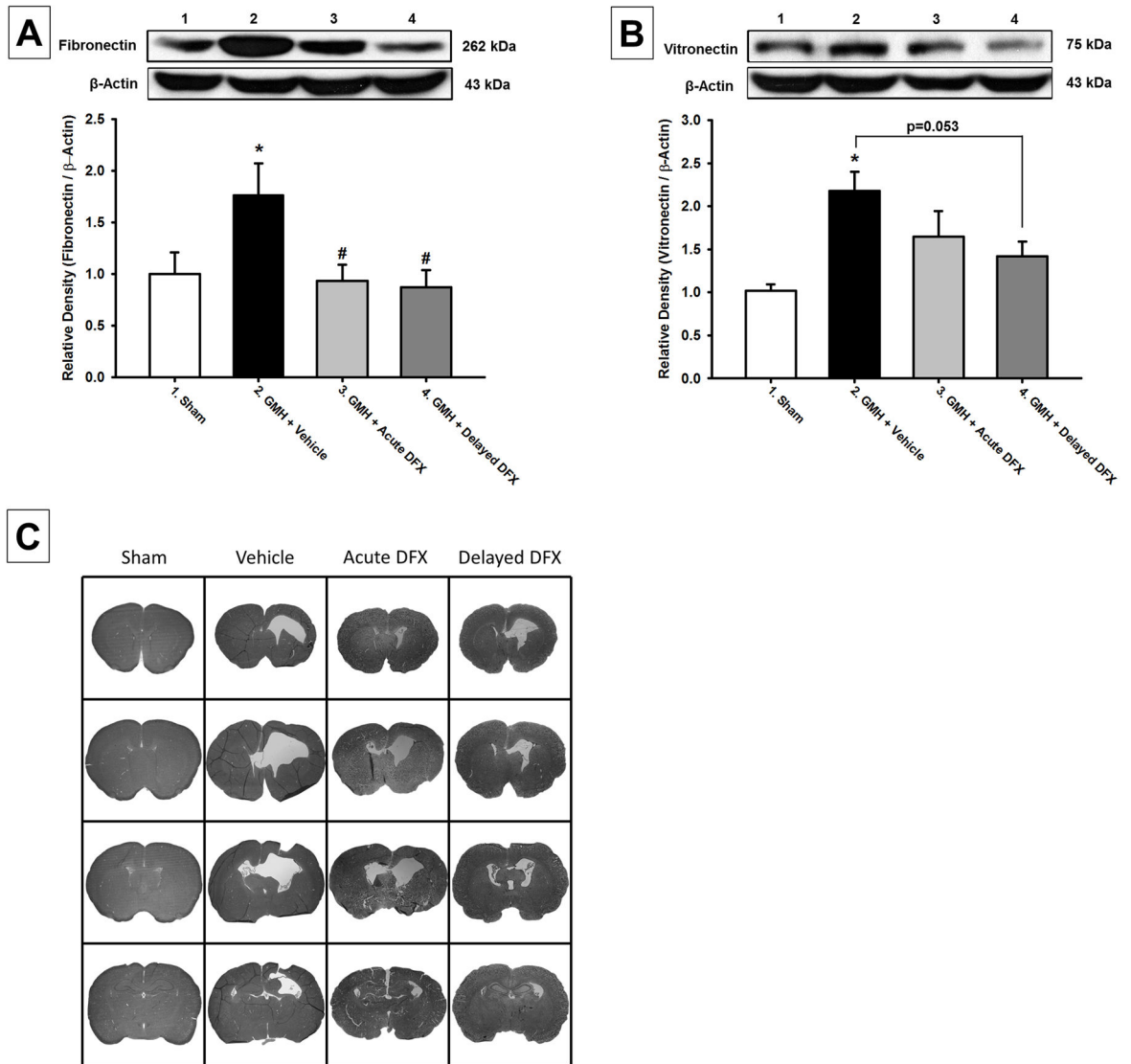


Figure 2. Western blot analysis of (A) Fibronectin and (B) Vitronectin at 28 days after germinal matrix hemorrhage. Representative microphotographs of Nissl stained brain sections (C) at 28 days after germinal matrix hemorrhage. Values are expressed as mean±SEM. *P<0.05 compared to sham, and #P<0.05 compared to vehicle. N=5 per group.

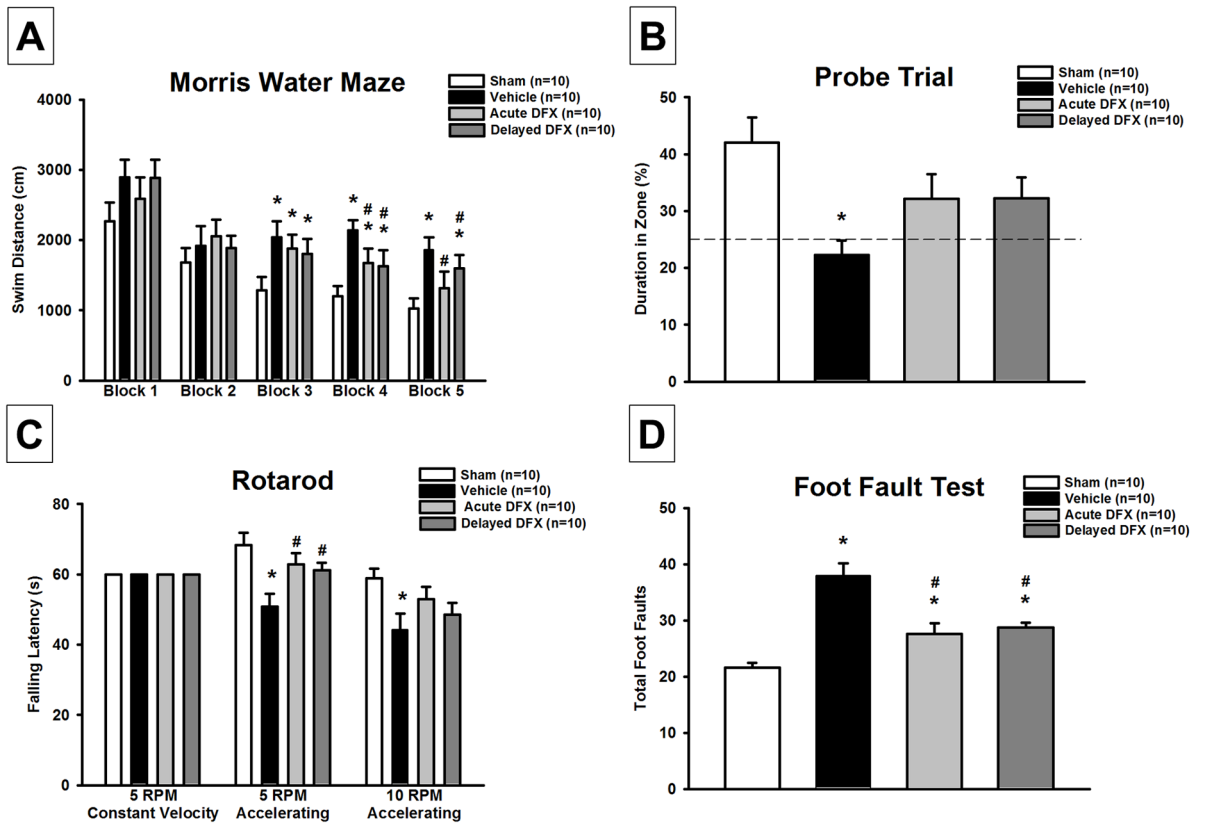


Figure 3. Neurofunctional assessment of (A) & (B) Morris water maze, (C) rotarod, and (D) foot fault test at 21–28 days after germinal matrix hemorrhage. Values are expressed as mean±SEM. *P<0.05 compared to sham, and #P<0.05 compared to vehicle. N=10 per group.